ELSEVIER

Alzheimer's & Dementia 8 (2012) S112–S121

Alzheimer's & Dementia

White matter imaging changes in subjective and mild cognitive impairment

Per Selnes[a,b,*], Anders M. Fjell[c,d], Leif Gjerstad[e], Atle Bjørnerud[f,g], Anders Wallin[h], Paulina Due-Tønnessen[f], Ramune Grambaite[a], Vidar Stenset[a,b], Tormod Fladby[a,b]

[a]*Department of Neurology, Faculty Division, Akershus University Hospital, University of Oslo, Lørenskog, Norway*
[b]*Department of Neurology, Akershus University Hospital, Lørenskog, Norway*
[c]*Department of Psychology, Center for the Study of Human Cognition, University of Oslo, Oslo, Norway*
[d]*Department of Neuropsychology, Oslo University Hospital, Ullevaal, Oslo, Norway*
[e]*Department of Neurology, Oslo University Hospital, Rikshospitalet, Oslo, Norway*
[f]*Department of Radiology, Oslo University Hospital, Rikshospitalet, Oslo, Norway*
[g]*Department of Physics, University of Oslo, Oslo, Norway*
[h]*Department of Neurochemistry and Psychiatry, Institute of Neuroscience and Physiology, Sahlgrenska Academy at Göteborg University, SU/Sahlgrenska, Gothenburg, Sweden*

Abstract

Background: To determine whether white matter (WM) memory network changes accompany early cognitive impairment and whether these changes represent early, pathologically independent axonal affection, we combined WM diffusion tensor imaging and cortical morphometric measurements of normal control subjects, patients with only subjective cognitive impairment (SCI), or mild cognitive impairment (MCI).

Methods: We included 66 patients with SCI or MCI and 21 control subjects from a university-hospital-based memory clinic in a cross-sectional study. Morphometric analysis was performed in FreeSurfer, and Tract-Based Spatial Statistics was used for analysis of diffusion tensor imaging-derived WM fractional anisotropy, radial diffusivity (DR), and mean diffusivity (MD). Relationships between WM measures and stage were assessed with whole-brain voxelwise statistics and on a region-of-interest basis, with subsequent correction for cortical atrophy.

Results: In SCI patients, as compared with control subjects, there were widespread changes in DR and MD. No significant differences in thickness could be demonstrated. In MCI patients, as compared with control subjects, there were widespread changes in DR, MD, and fractional anisotropy; the precuneal and inferior parietal cortices were thinner; and the hippocampus was smaller. Multiple logistic regression analysis eliminated morphometry as an explanatory variable in favor of DR/MD for all regions of interest, except in the precuneus, where both thickness and DR/MD were significant explanatory variables.

Conclusions: WM tract degeneration is prominent in SCI and MCI patients, and is at least in part independent of overlying gray matter atrophy.

Keywords: Alzheimer's disease; Subjective cognitive impairment; Mild cognitive impairment; Diffusion tensor imaging; Volumetric MRI; White matter

1. Background

Characterization of predementia stages is necessary to understand early mechanisms for dementia development. Mild cognitive impairment (MCI) is a clinical condition associated with an increased risk of dementia [1,2]. From clinical normalcy to dementia, there is a broad range of pathological affection, but the majority of MCI cases have

The authors have no conflicts of interest to report.

V.S. is currently at the Department of Neurosurgery, Oslo University Hospital, Ullevaal, 0450 Oslo, Norway.

*Corresponding author. Tel.: +47 02900; Fax: +47 67968132.

E-mail address: per.selnes@medisin.uio.no

1552-5260/$ - see front matter © 2012 The Alzheimer's Association. All rights reserved.
doi:10.1016/j.jalz.2011.07.001

recently been shown to have Braak stage III or more extensive neurofibrillary changes, at least a moderate amount of amyloid plaques already consistent with a diagnosis of Alzheimer's disease (AD), and frequently also destruction of essential parts of the medial temporal lobe [3,4]. Thus, intervention (to stop or postpone dementia development) before extensive central nervous system damage necessitates in vivo characterization of a pre-MCI condition [5]. Criteria for earlier cases with less advanced affection have been proposed, for example, the Global Deterioration Scale (GDS) [6,7], where stage 2 corresponds to a stage less advanced than MCI, which is subjective cognitive impairment (SCI) [8]. Clinical investigation of SCI patients does not reveal cognitive impairment, and these patients score according to norms on screening tests, whereas criteria for MCI encompass cognitive impairment [1]. The SCI group is less studied and probably even more heterogeneous than MCI. However, SCI is regarded as a pre-AD stage [8], and is also associated with an increased risk of dementia [8,9], but the extent of AD-related changes or other types of pathology (e.g., small-vessel disease, as has been shown for some MCI subjects [5]) is unknown.

Braak stage I entorhinal neurofibrillary changes have been identified in young cognitively normal individuals [3]. Although the natural evolution of these changes is not fully understood, they correlate with the degree and presence of dementia [10], and their roots can be traced to several decades before clinical AD [11]. Specific loss of layer II entorhinal cortex neurons seems to occur in very mild AD [12]. As also seen on magnetic resonance imaging (MRI) and positron emission tomography acquisitions, AD is characterized by a sequential and specific pattern of cerebral atrophy and hypometabolism [13,14], and the alterations in MCI are in particular found in temporal and parietal areas comprising the hippocampus, entorhinal, parahippocampal, retrosplenial, posterior cingulate, precuneus, supramarginal, inferior parietal, and middle temporal cortices [15]. During the later stages of AD, this pathology is even more widespread, with severe destruction of isocortical association areas as a key feature [3].

Several studies have shown distinct patterns of atrophy in normal aging [16] and AD [14] by using structural MRI to quantify cortical and subcortical structures. Long myelinated axonal projections connecting cortical and subcortical regions are main constituents of cerebral white matter (WM). Diffusion tensor imaging (DTI) measures a diffusion tensor that (for each voxel) is represented by three eigenvectors with corresponding eigenvalues that define an ellipsoid. Because the diffusion of water molecules will be more pronounced parallel (or axial) to, rather than perpendicular (or radial) to, WM tracts, magnetic resonance DTI can thus be used to provide different indices of the microstructural integrity of the axonal bundles, such as fractional anisotropy (FA), axial diffusivity (DA), radial diffusivity (DR), and mean diffusivity (MD). FA is frequently used and expresses the proportion of axial-to-radial diffusion, that is, how directional the water diffusion is within a given voxel [17]. DR is a measure of the degree of restriction due to membranes, myelin, and other effects (see later in the text). There are, however, challenges in interpreting DTI measurements because their relation to different types of pathology is not clear-cut. Increased DR has been associated with myelin damage [18], but a nearly complete lack of myelin in the examined mice only resulted in a 20% increase in DR, pointing toward the importance of factors other than myelin [19]. DA seems to increase after corpus callosotomy, but this is transient and followed by a longer-term decrease [20].

Although the neuropathological diagnosis of AD is still based on the presence of primarily cortical alterations, widespread WM disease is reported to be prominent in neuropathological studies of AD patients [21]. Also, profound alterations in the perforant pathway (effectively disconnecting the hippocampal formation from the association and limbic cortices) have been reported [22]. DTI WM changes in AD and MCI are far less studied than structural changes (but refer to [23,24]). Previously we found that WM FA is more sensitive than WM volume to changes in WM integrity during middle age [25]. Although few studies have investigated the relationship between gray matter structures and connecting WM tracts, Salat et al [26] reported parahippocampal WM changes in AD partly independent of gray matter degeneration, as measured by hippocampal volume.

In the present study, we wanted to answer the following three questions: (1) Do changes in WM diffusivity occur in the early stages of cognitive impairment? (2) Could these putative changes in diffusivity represent pathological processes independent of gray matter atrophy? (3) How do the different DTI indices compare with each other and with cortical atrophy, as measured by morphometry, in terms of identifying pathological alterations in early cognitive impairment? To answer these questions, WM tract diffusivity for patients presenting with either SCI or MCI was compared with that for age-matched cognitively normal control subjects, and DTI findings were compared with morphometric changes.

2. Methods and study subjects

2.1. Eligibility criteria, measures of cognitive impairment, and ethical conduct

Cognitively impaired patients with spouses were recruited consecutively from a university-hospital-based memory clinic during approximately 4 years. Inclusion criteria for all groups were age 45 to 79 years and established normality or impaired cognition for at least 6 months. All patients had subjective cognitive complaints, whereas control subjects did not. SCI and MCI are largely congruent with and herein defined as the second (SCI) and third (MCI) stages of the GDS [6,7]. GDS stage was determined from a clinical interview and the following screening

tests: Mini-Mental State Examination [27], stepwise comparative status analysis parameters 13–20 [28], I-Flex (fluency, interference, and numeral–letter items) [29], and Cognistat [30], which screen among others memory (including cued recall) and executive functions. To further ensure that the patients were not demented, the Clinical Dementia Rating [31] was administered. To be classified as GDS 2 (SCI), patients had to score above cutoff on all screening tests; patients scoring below were classified as GDS 3 (MCI). Patients scoring GDS >3, Clinical Dementia Rating >0.5, or >1 (in sum) of stepwise comparative status analysis variables 13–20 were considered demented and not included. Spouses of participating patients were potentially eligible as control subjects, provided they had a GDS score of 1, that is, clinically established normality with regard to memory, emotionality, and tempo. The GDS scores for control subjects were determined solely by a clinical interview, but, subsequently, putative control cases had neuropsychological testing performed, and were only included if they had a T-score of ≥40 on verbal learning and memory. Patients also underwent these neuropsychological tests (Table 1). This method of determining GDS stage is in agreement with a previously used method [32].

Exclusion criteria were impaired activities of daily living, established psychiatric disorder, cancer, drug abuse, solvent exposure, and anoxic brain damage.

The South-Eastern Norway ethical committee for medical research had no objections to the study protocol, and informed consent was obtained from all subjects before any study-specific procedures were performed.

2.2. MRI/DTI acquisition

MRI scans were obtained from two sites. In site 1, we used a Siemens Symphony 1.5 T (Siemens Medical Solutions, Erlangen, Germany) with a conventional quadrature head coil and a magnetic resonance technique that uses a rapid gradient echo sequence preceded by magnetization preparation pulses (magnetization-prepared rapid gradient echo [MP-RAGE]). Two three-dimensional MP-RAGE T1-weighted sequences were obtained in succession (repetition time [TR]/echo time [TE]/inversion time/flip angle = 2730 ms/3.19 ms/1100 ms/15°, matrix = 256 × 192, 128 sagittal slices, thickness = 1.33 mm, in-plane resolution of 1.0 mm × 1.33 mm). In site 2, we used Siemens Espree 1.5 T. One three-dimensional MP-RAGE T1-weighted sequence was obtained (TR/TE/inversion time/flip angle = 2400/3.65/1000/8°, matrix = 240 × 192, 160 sagittal slices, thickness=1.2 mm, in-plane resolution of 1 mm×1.2 mm).

The pulse sequences for DTI at the two sites were as follows: site 1: b = 700, 12 directions repeated twice, one b0-value per slice, TR = 4300 ms, TE = 131 ms, number of axial slices = 19, slice thickness = 5 mm (gap = 1.5 mm), in-plane resolution = 1.8 × 1.8 mm^2, bandwidth = 955 Hz/pixel; and site 2: b = 750, 12 directions repeated 5 times, five b0-values per slice, TR = 6100 ms, TE = 117 ms, number

Table 1
Demographic information, results of cognitive tests, and mean values of parameters of morphometry/DTI*

Variables	MCI N = 50	SCI N = 16	Normal control subjects N = 21
Age; mean (Range)†	61.2 (45–77)	59.2 (45–71)	62.0 (49–77)
Men/Women‡	26/24	5/11	5/16
MRI site 1/site 2‡	15/35	4/12	7/14
MMSE; total§	27.6	28.9	29.5
RAVLT Learning T-score (SD)§	41.1 (13.6)	48.1 (11.0)	55.8 (8.6)
RAVLT Delayed recall T-score (SD)§	41.6 (12.4)	48.7 (9.4)	54.2 (7.3)
Global Deterioration Scale score	3	2	1
STEP; variables 13–20	≤1	0	NA
Clinical dementia rating; global score	0.5	≤0.5	NA
Entorhinal Th/FA/MD/DR	3.42/0.30/88.0/75.0	3.33/0.31/88.1/74.3	3.58/0.31/81.6/68.7
Parahippocampal Th/FA/MD/DR	2.58/0.35/89.9/73.7	2.61/0.35/87.9/71.7	2.73/0.37/82.2/66.2
Retrosplenial Th/FA/MD/DR	2.42/0.54/79.1/51.9	2.47/0.55/79.4/51.7	2.51/0.56/75.4/47.7
Posterior cingulate Th/FA/MD/DR	2.41/0.53/85.7/58.3	2.45/0.54/85.9/57.5	2.48/0.56/82.5/53.6
Precuneus Th/FA/MD/DR	2.10/0.41/84.2/64.9	2.14/0.42/83.4/63.8	2.25/0.44/79.5/59.7
Inferior parietal Th/FA/MD/DR	2.27/0.37/88.4/71.7	2.32/0.37/87.1/70.4	2.41/0.38/83.1/66.3
Supramarginal Th/FA/MD/DR	2.29/0.35/83.6/68.6	2.36/0.36/81.7/66.6	2.41/0.37/78.4/63.4
Middle temporal Th/FA/MD/DR	2.81/0.38/85.6/68.3	2.76/0.39/84.6/66.8	2.89/0.40/80.0/62.7
Hippocampal volume in mL	3.89	3.92	4.04

Abbreviations: DTI, diffusion tensor imaging; MCI, mild cognitive impairment; SCI, subjective cognitive impairment; MMSE, Mini-Mental State Examination; RAVLT, Rey Auditory Verbal Learning Test; SD, standard deviation; STEP, stepwise comparative status analysis; Th, thickness in mm; FA, fractional anisotropy; MD, mean diffusivity; DR, radial diffusivity; NA, not applicable.

*Mean values for cortical thickness and from tracts in white matter underlying the cortical regions of interest.

†T-tests do not show significant differences in age between groups.

‡χ^2 tests do not show any significant differences in age, sex, or MRI site distribution between the groups.

§T-tests show significant differences between control subjects and SCI patients ($P \leq .05$), and between control subjects and MCI patients ($P < .001$). For comparison of imaging variables between groups, please refer to Table 2.

of slices = 30, slice thickness = 3 mm (gap = 1.9 mm), in-plane resolution = 1.2 × 1.2 mm^2, bandwidth = 840 Hz/pixel. Most MRI scans were obtained from site 2 (14 control subjects and 47 patients).

As described in another publication on a subsample from this study [33], six of the included control subjects were scanned on both scanners and volumes of hippocampus, cortex, and the lateral ventricles were estimated and correlated across scanners. The Pearson coefficients were 0.99, 0.90, and 0.999, respectively (all P values $<.05$). Mean differences in cortical thickness were generally within ± 0.1 mm across the brain surface. This indicates that change of scanner did not introduce much bias in the structural data.

2.3. MRI segmentations and analyses

Cortical reconstruction and volumetric segmentation were performed with the FreeSurfer image analysis suite version 4.5.0 (Massachusetts General Hospital, Boston, MA). This includes segmentation of the subcortical WM and deep gray matter volumetric structures [34] and parcellation of the cortical surface [35] according to a previously published parcellation scheme [36]. This labels cortical sulci and gyri, and thickness values are calculated in the regions of interest (ROIs). Based on the cortical parcellation, WM in the gyrus underneath each cortical label was identified. Each WM voxel within a gyrus was labeled according to the label of the nearest cortical voxel. Deep WM was not assigned to a particular cortical area, with a 5-mm distance limit.

The Oxford Centre for Functional MRI of the Brain (FMRIB) Software Library (FSL) version 4.1 [37,38] was used for DTI analyses and calculations. Initially, FMRIB's Linear Image Registration Tool [39] was used for affine registrations of each DTI volume to the low-b (b = 0) image. Motion between scans and residual eddy currents were corrected for, before creation of FA and eigenvalue maps. DR was defined as the mean of eigenvalues 2 and 3, and MD as the mean of all three eigenvalues. Tract-Based Spatial Statistics [17] (part of FSL) was used for voxelwise statistical analysis of the DTI variables (FA, DR, and MD). FMRIB's Diffusion Toolbox was used to create FA images by fitting a tensor model to the raw diffusion data, and FSL's Brain Extraction Tool was used for subsequent brain extraction. All subjects' FA data were then aligned into a common space using the nonlinear registration tool FMRIB's Nonlinear Image Registration Tool, which uses a B-spline representation of the registration warp field [40]. Next, the mean FA image was created and thinned to create a mean FA skeleton that represents the centers of all tracts common to the group. Each subject's aligned FA data were then projected onto this skeleton and the resulting data fed into voxelwise cross-subject statistics. DR and MD data were then extracted from each subject according to the skeletonized FA map. Moreover, WM ROIs based on the FreeSurfer WM parcellations were extracted for FA, DR, and MD; the FSL FMRIB58_FA template (to which every subject's FA volume initially was registered) was coregistered to the standard space T1 volume MNI152, which subsequently went through the FreeSurfer processing stream to create a volume with WM parcellations. The registration between the FA template and the MNI152 volume was applied to the volume with the WM parcellations, and the resulting volume was used to extract the skeletonized FA, DR, and MD data from each WM ROI. Pearson correlations between the thickness of each ROI and the DTI variables in the underlying WM were determined.

2.4. Regions of interest

The hippocampus, entorhinal, parahippocampal, retrosplenial, posterior cingulate, precuneus, inferior parietal, supramarginal, and middle temporal cortices, and the underlying WM were chosen as ROIs. This choice is accounted for in a previous publication on a subset of this material [15] and was motivated by previously documented alterations within these integral parts of the episodic memory network in MCI. ROIs were averaged across hemispheres to reduce the number of statistical operations.

2.5. Statistics

PASW 18 (SPSS Inc., Chicago, IL) was used for ROI-based statistical analyses. To obtain optimal accuracy, the morphometric variables were corrected for the (significant) effects of age and sex (for the hippocampus, also intracranial volume) by regression. This yielded standardized residuals for further use. The DTI variables were likewise corrected for age, sex, and scanner site. Univariate 1-way analyses of variance with Bonferroni correction post hoc were then used to test whether (the means of) the standardized MRI variables were different between normal control subjects and the SCI and MCI groups.

Whole-brain voxelwise statistics were performed using Randomise from the FSL suite, with threshold-free cluster enhancement (TFCE) [41] to correct for multiple comparisons. The threshold was set at $P < .05$. Scanner, age, and sex were treated as nuisance variables.

Multiple logistic regression analysis was performed with control/MCI as the dependent variable and thickness and in turn each of the corresponding DTI variables (DR, FA, MD) for each of the chosen ROIs as simultaneous explanatory variables. Pearson correlations were determined for each ROI between thickness and each of the DTI variables, and between the ROIs within each modality. We also compared the different diffusion tensor properties and morphometry in terms of diagnostic power by constructing receiver operating characteristic curves for the different modalities' abilities to discriminate between MCI patients and control subjects. Further, the Pearson correlations between the different ROIs within the same modalities were examined (e.g., the correlation between entorhinal thickness and retrosplenial thickness).

2.6. Checking results in native space

To confirm that the voxels in the FA skeleton that had a significantly different DR actually were derived from the correct tract-center points in all subjects, these voxels were projected back from their position on the skeleton to the nearby position at the center of the nearest tract in the subject's FA image in standard space (i.e., after the FA image had been nonlinearly registered to the target image). Further, these points were then "inversely warped" back into the subject's native space by inverting the nonlinear registration that was originally applied. The voxels were then manually inspected in both standard and native space. There was a generally satisfactory overlap between tract centers and back-projected voxels. This procedure was also performed for the mean FA skeleton, and manual inspection confirmed that the voxels in the mean FA skeleton actually were derived from tract-center points. Further, the selected WM ROIs from the FreeSurfer parcellation of the standard space T1 volume MNI152 were also projected back to both standard and native space and manually inspected for accuracy.

2.7. Study subjects

In all, 21 control subjects and 66 patients were enrolled in the study and subjected to MRI. All patients had been referred to the university-based memory clinic for memory complaints. Figure 1 shows exclusions and inclusions in the according-to-protocol cohorts, and Table 1 presents subject characteristics, results of cognitive tests, and mean MRI indices.

3. Results

3.1. WM and gray matter changes in SCI and MCI

None of the nine ROIs assessed were significantly thinner, but the tracts in WM underlying the posterior cingulate, retrosplenial, and middle temporal cortices had significantly higher DR and MD in the SCI group than in control subjects (Table 2) (as determined by the ROI-based analysis with Bonferroni post hoc correction). Tracts underlying the precuneus had significantly higher DR and lower FA, and parahippocampal tracts had lower FA. Widespread tracts in the SCI group had significantly different DR and MD, but not

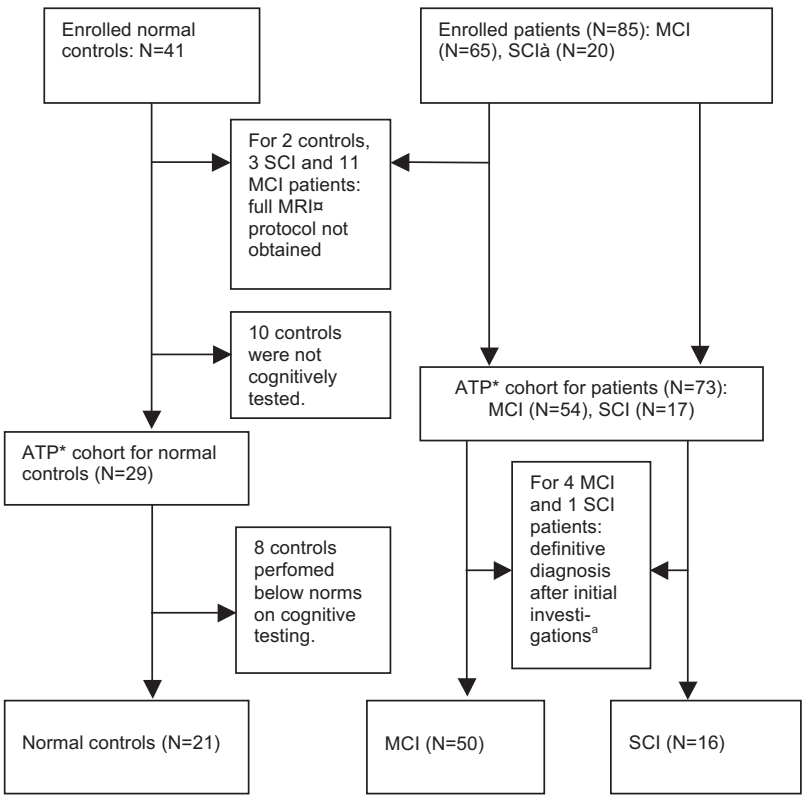

[a]Diagnoses: Normal pressure hydrocephalus, Lewy body disease, frontotemporal dementia. *ATP-according to protocol. Mild cognitive impairment. àSubjective cognitive impairment. ¤Magnetic resonance imaging.

Fig. 1. Exclusions and inclusions in the according-to-protocol cohorts. [a]Diagnoses: Normal pressure hydrocephalus, Lewy body disease, frontotemporal dementia. *According-to-protocol. [†]Mild cognitive impairment. [‡]Subjective cognitive impairment. [§]Magnetic resonance imaging.

Table 2
Relations between extent of cognitive impairment and parameters of morphometry/DTI, as assessed by Bonferroni post hoc analysis of variance

		Parameters of DTI									Morphometry		
		DR†			FA†			MD†			Th†		
ROI	Group*	SE‡	*P*	Mean Dif.‡	SE‡	*P*	Mean Dif.‡	SE‡	*P*	Mean Dif.‡	SE‡	*P*	Mean Dif.‡
Entorhinal	SCI	0.32	.167	−0.62	0.33	1.00	0.17	0.32	.095	−0.69	0.32	.066	0.75
	MCI	0.25	.074	−0.57	0.26	.444	0.37	0.25	.063	−0.59	0.25	.387	0.39
Parahippocampal	SCI	0.31	.062	−0.74	0.32	**.033**	0.82	0.31	.059	−0.74	0.33	.468	0.47
	MCI	0.25	**.014**	−0.71	0.25	.137	0.50	0.24	**.009**	−0.75	0.26	.628	0.32
Retrosplenial	SCI	0.30	**.004**	−1.0	0.31	.053	0.76	0.30	**.001**	−1.11	0.33	1.00	0.28
	MCI	0.24	**.001**	−0.92	0.25	**.028**	0.66	0.23	**.000**	−0.93	0.26	.526	0.35
Posterior cingulate	SCI	0.31	**.029**	−0.82	0.31	.092	0.69	0.31	**.022**	−0.86	0.33	.936	0.33
	MCI	0.24	**.008**	−0.76	0.24	**.009**	0.75	0.24	**.026**	−0.66	0.26	.405	0.39
Precuneus	SCI	0.31	**.047**	−0.77	0.31	**.037**	0.80	0.31	.054	−0.75	0.31	.069	0.73
	MCI	0.24	**.007**	−0.77	0.24	**.011**	0.73	0.24	**.007**	−0.76	0.25	**.007**	0.77
Inferior parietal	SCI	0.32	.118	−0.66	0.32	.079	0.72	0.32	.141	−0.63	0.32	.138	0.65
	MCI	0.25	**.028**	−0.66	0.25	.123	0.52	0.25	**.021**	−0.68	0.25	**.037**	0.64
Supramarginal	SCI	0.31	.157	−0.61	0.32	.081	0.71	0.31	.187	−0.59	0.32	.640	0.41
	MCI	0.24	**.004**	−0.80	0.25	**.037**	0.63	0.24	**.006**	−0.78	0.25	.139	0.51
Middle temporal	SCI	0.30	**.022**	−0.83	0.32	.168	0.61	0.30	**.012**	−0.89	0.32	.068	0.75
	MCI	0.24	**.000**	−0.94	0.25	**.021**	0.68	0.24	**.000**	−0.95	0.25	.673	0.31
Hippocampus	SCI	NA			NA			NA			0.32	.182	0.60
	MCI										0.25	**.045**	0.62

Abbreviation: ROI, region of interest.

NOTE. There were no statistically significant differences in parameters of morphometry/DTI between the SCI and the MCI groups. Significant *P* values are shown in bold.

*Each group has been compared with normal control subjects.

†Dependent variables. For the hippocampus, the dependent variable is volume.

‡SE and mean difference are in standard deviations.

FA, from those in the control group (as determined by whole-brain voxelwise statistics on the diffusion data, with TFCE correction for multiple comparisons). Further, the precuneal and inferior parietal cortices were significantly thinner in the MCI group than in control subjects. The hippocampus was significantly smaller in MCI, but not in SCI, when compared with control subjects.

DR and MD were significantly higher for MCI patients than control subjects in all ROIs (except in the entorhinal cortex). For FA, there were significant differences between control subjects and MCI patients for the tracts underlying the retrosplenial, posterior cingulate, precuneal, supramarginal, and middle temporal cortices.

There were no statistically significant differences between the SCI and the MCI groups.

For whole-brain voxelwise statistics with TFCE, there were widespread differences in DR, FA, and MD between MCI patients and control subjects, and widespread differences in DR and MD (but not FA) between SCI patients and control subjects. Figure 2 shows the statistical map of the differences in DR, FA, and MD between patients and control subjects.

3.2. Relations between measures of gray matter and WM changes

Multiple logistic regression analysis eliminated most of the morphometric variables when coanalyzed with the corresponding DR variable. The DR and MD variables were significant for all ROIs, whereas FA was significant for several ROIs. Only precuneal thickness was significant when included in the same regression analysis as its corresponding DR and MD variable (Table 3).

The correlations between thickness of the posterior cingulate and the DTI variables were weak (0–0.1 for DR, FA, and MD). The correlations between thickness and FA for the other ROIs were in general weaker (mean correlation = 0.18) than between thickness and the other DTI variables (−0.33 for both DR and MD).

Figure 3 presents receiver operating characteristic curves. Both DR and MD discriminate better between MCI patients and control subjects than morphometry. DR and MD were best for all applicable ROIs, and areas under the curve were very similar for these two indices. FA was slightly better than morphometry. Mean areas under the curve were 0.64 for morphometry, 0.74 for DR, 0.68 for FA, and 0.75 for MD.

The Pearson correlations between the different ROIs within the same modalities were generally strong (mean correlation: 0.51 for morphometry, 0.58 for DR, 0.63 for FA, and 0.53 for MD).

4. Discussion

4.1. WM diffusivity network changes

DTI measurements show affection of subcortical WM in SCI and (more pronounced) in MCI patients. The results

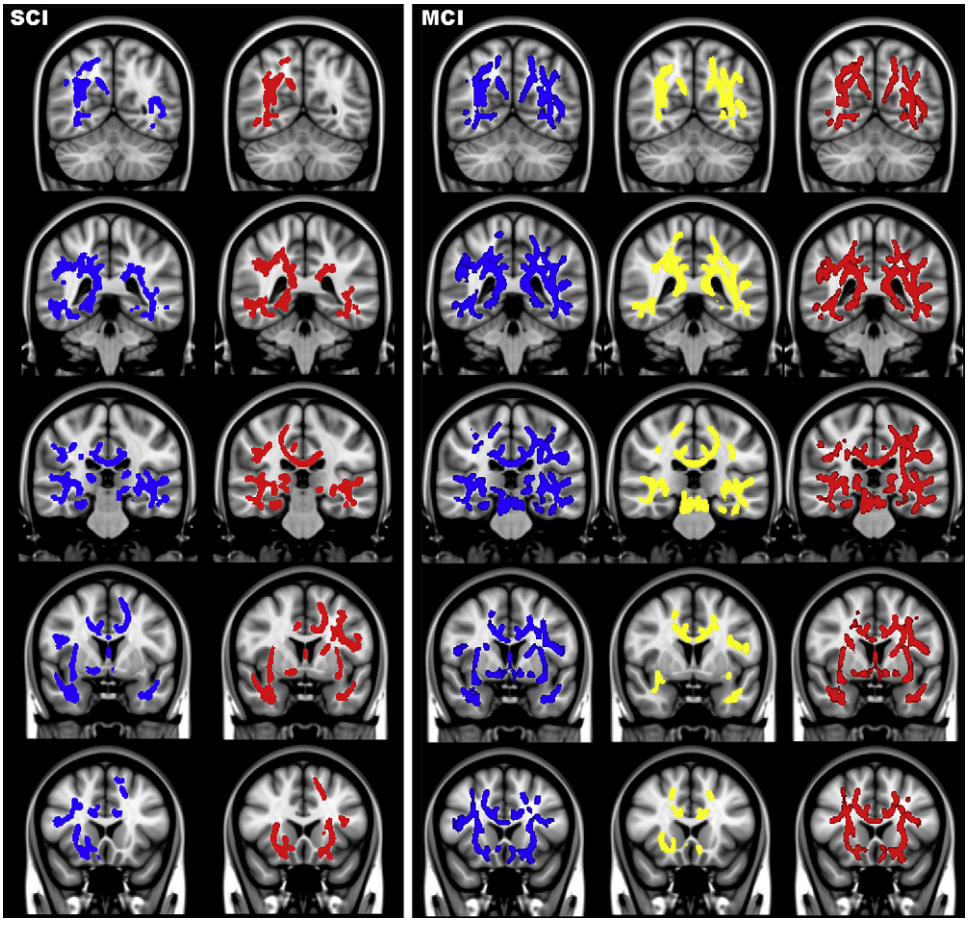

Fig. 2. Whole-brain voxelwise diffusion tensor imaging statistics. The statistical map (shown in blue for radial diffusivity [DR], yellow for fractional anisotropy [FA], and red for mean diffusivity [MD]) represents voxels in the FA skeleton for which DR, FA, and MD are significantly higher in patients than in control subjects. The map for subjective cognitive impairment is shown to the left, with mild cognitive impairment to the right. For FA, no voxels were significantly different between subjective cognitive impairment patients and control subjects. Multiple comparisons were corrected for by threshold-free cluster enhancement. The threshold was set at $P < .05$.

suggest that both the medial temporal and the cingulate regions may be affected at the SCI stage. This interpretation is supported by the overlapping, but more extensive, affection of adjacent WM and cortical regions that we see at the MCI stage (encompassing a.o. middle temporal and cingulate parietal DTI indices, precuneal and inferior parietal cortical thickness, as well as hippocampal atrophy, in addition to the affection present at the SCI stage). We thus confirm our previous findings of early WM cingulate affection [42], but by using Tract-Based Spatial Statistics, which is a non-ROI-based method, for evaluation of WM tract integrity. The pattern of atrophy (e.g., hippocampus and precuneal cortex) in the MCI group is reminiscent of more fully developed AD pathology, and also overlaps with the DTI changes in the SCI group. The etiology of these early changes is not established, and may hypothetically involve both vascular disease [43] and endogenous neuronal factors such as tau and amyloid pathology [44].

Although both are parts of the memory network, the cingulate and medial temporal lobe are anatomically distant. In the monkey, reciprocal, but weak, connections have been reported [45]. Thus, the combined affection of these areas is more consistent with distributed, rather than localized, disease, also at this early stage. Although we cannot demonstrate entorhinal changes in the ROI-based analyses, there are prominent medial temporal WM changes in the whole-brain analyses. This discrepancy may possibly be explained by the 5-mm distance limit (ensuring relation between cortex and labeled WM), the relatively minute structures in question, and the resolution of the scans, leaving a limited number of labeled voxels. Entorhinal affection is well documented in postmortem pathological studies of early and preclinical cases as well as the normal population [3], whereas a putative early affection of the cingulate cortex [42] is less well documented. Thus, these findings need independent confirmation and eventual correlation to pathological observations.

WM changes corresponding to the cingulate complex appear to involve the posterior cingulate, retrosplenial, and precuneus already at the SCI stage, and more pronounced at the MCI stage.

Table 3
Logistic regression*; regional thickness and DTI measures

ROI, regression coefficient (B) and associated *P* value	DR versus Th		FA versus Th		MD versus Th	
	DR	Th	FA	Th	MD	Th
Entorhinal						
B	−1.04	0.55	0.37	0.64	−1.13	0.54
P	**.024**	.133	.200	.061	**.017**	.148
Parahippocampal						
B	−1.73	0.07	0.69	0.33	−1.95	0.03
P	**.002**	.824	**.031**	.247	**.002**	.937
Retrosplenial						
B	−1.61	0.18	0.99	0.25	−1.42	0.19
P	**.000**	.540	**.010**	.363	**.000**	.531
Posterior cingulate						
B	−1.07	0.37	0.94	0.34	−0.99	0.42
P	**.004**	.197	**.007**	.224	**.006**	.135
Precuneus						
B	−1.17	0.71	0.83	0.78	−1.15	0.77
P	**.014**	**.042**	**.022**	**.023**	**.012**	**.026**
Inferior parietal						
B	−0.89	0.58	0.64	0.71	−0.90	0.58
P	**.033**	.082	.053	**.027**	**.029**	.084
Supramarginal						
B	−0.98	0.33	0.72	0.45	−0.95	0.35
P	**.009**	.280	**.023**	.138	**.011**	.252
Middle temporal						
B	−1.54	0.40	0.84	0.61	−1.65	0.40
P	**.001**	.363	**.012**	.119	**.001**	.376

NOTE. Significant *P* values are shown in bold.
*MCI/control as the dependent variable, and Th and DR/FA/MD as explanatory variables.

Neither at the SCI nor at the MCI stage were significant thickness differences in the posterior cingulate found in the present sample. This is also reflected in the weak correlations between thickness of this ROI and the DTI variables. Larger studies using similar segmentation methods have previously found group effects in this area [46], and trend-level differences have also been observed in an overlapping sample from the present study [15]. Still, it is interesting that even in the absence of a significant group difference in cortical thickness in the posterior cingulate, significant differences in DTI parameters were observed.

Although there were no significant differences between the SCI and MCI groups, the mean values of the imaging parameters were in general between the control and the MCI groups, supporting the view of SCI as a transitional stage between normality and MCI. A limitation, however, is the relatively small SCI sample size.

Other limitations of the study that should be emphasized include the heterogeneous nature of the clinical categories SCI and MCI, also due to the low age inclusion limit. Conceivably, the WM changes (particularly in the SCI group) could in part be related to, for example, subclinical depression, which cannot be excluded as a contributing factor to cognitive impairment even after the screening and diagnostic procedures performed (Fig. 1). Further, the ROI-based findings depend on the algorithm for automated parcellation, and chosen boundaries in the tissue may both be too crude and/or not necessarily correspond to biological boundaries of tissue affection. The present methodology also does not allow inferences about pathological predilection for certain types of fibers (e.g., association fibers more affected than projection or brainstem fibers), but this will be addressed in a planned future work.

4.2. Relations between gray matter and WM changes

Hypothetically, both cortical volume loss and corresponding loss of WM integrity may locally be part of the same process, neuronal degeneration affecting both somatic and axonal compartments. Nonetheless, as effects of DTI measures tend to remain after regressing out cortical thickness, the pattern of affection provides structural underpinnings to suggestions of early axonal affection in AD [47], also showing the importance of DTI measures other than FA. As the changes occur in several brain regions subserving memory, both in the medial temporal and cingulate complexes, this suggests a distributed process of degeneration, with predominant WM affection at the predementia stage. The cross-sectional nature of the present findings limits interpretations as to a putative sequential nature of regional affection, but these questions will be addressed in an ongoing longitudinal study in the same study population.

4.3. Comparisons between DTI indices and morphometry

As there seems to be a biphasic increase–decrease in DA, as previously reported [20], especially in chronic degenerative disorders, this causes problems for the interpretability of DA parameters because adjacent fibers may be in different phases of axial increase or decrease at the time of scanning [25]. If there is a simultaneous increase in both DA and DR, it follows from the definition of FA that the change in FA, contributed to by each, will cancel each other out (the proportion of axial-to-radial diffusion may be unchanged). Increased DR in AD pathology is expected, but reports of simultaneous increase in DA have been presented [24,26,48]. Thus, the biphasic increase–decrease in DA may render FA a less suitable DTI parameter than DR. This may especially be the case in early cognitive impairment, in which WM pathology is just starting to emerge. This is in accord with our finding that FA performs worse than DR and MD in uncovering changes in early cognitive impairment.

In conclusion: (1) WM diffusivity memory network changes are prominent already at the SCI stage and are overlapping, but more profound, at the MCI stage. (2) WM diffusivity changes remain after correction for cortical thickness and are at least in part independent of overlying gray matter pathology (as measured by structural MRI). (3) The WM diffusivity parameters DR and MD could better discriminate between patient groups with varying degrees of cognitive impairment than morphometry and FA.

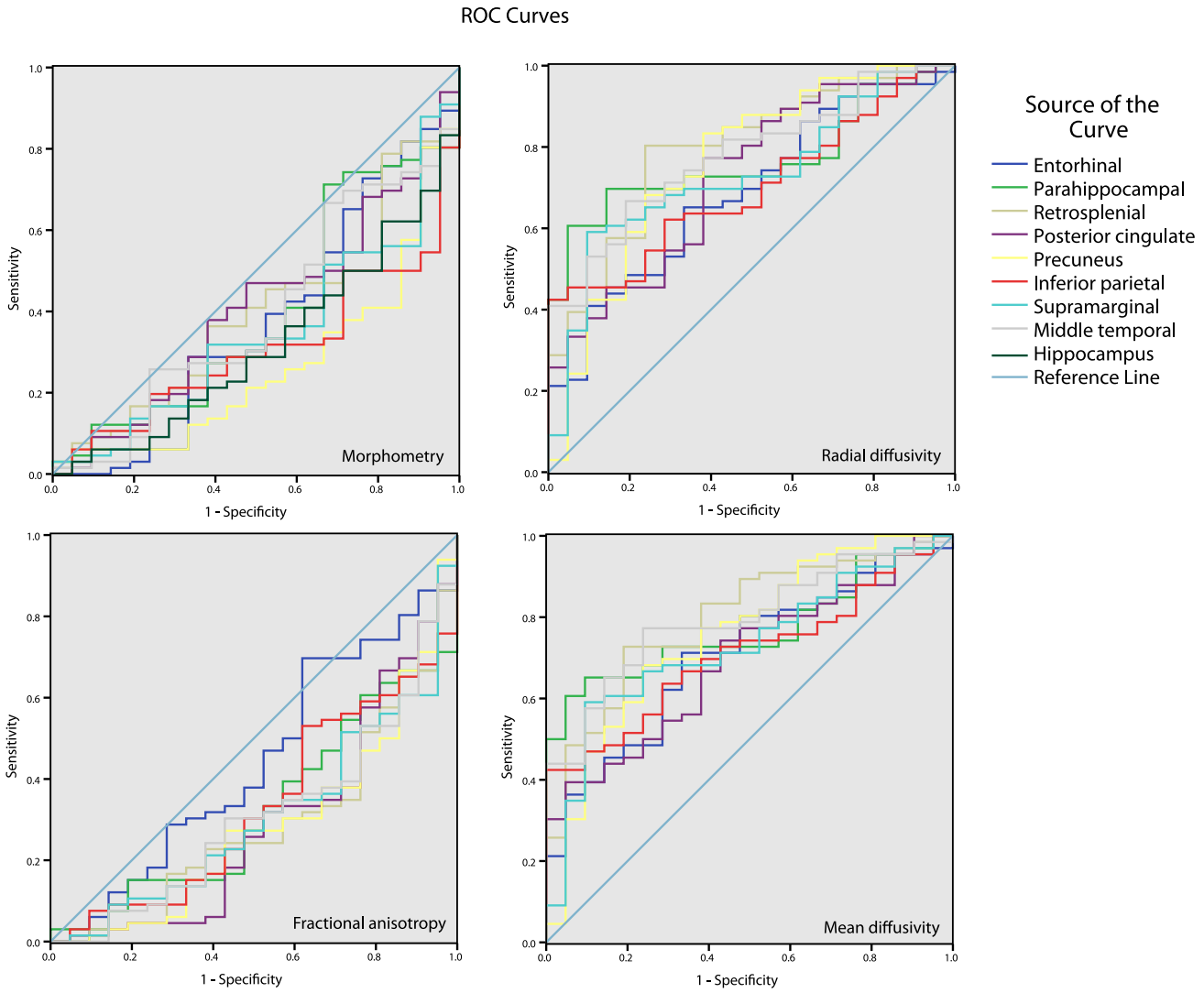

Fig. 3. Receiver operating characteristic curves. Receiver operating characteristic curves plotting true versus false positives as the discrimination thresholds for the different modalities are varied. Mean areas under the curve were as follows: morphometry, 0.64; DR, 0.74; FA, 0.68; and MD, 0.75.

Acknowledgments

This study has received supporting grants from The Research Council of Norway and South-Eastern Norway Regional Health Authority (Helse Sør-Øst). The authors thank medical writer Kari Skinningsrud (Limwric as, Norway) for substantive editing of the manuscript.

References

[1] Petersen RC. Mild cognitive impairment as a diagnostic entity. J Intern Med 2004;256:183–94.
[2] Petersen RC, Jack CR Jr. Imaging and biomarkers in early Alzheimer's disease and mild cognitive impairment. Clin Pharmacol Ther 2009; 86:438–41.
[3] Braak H, Braak E. Evolution of the neuropathology of Alzheimer's disease. Acta Neurol Scand Suppl 1996;165:3–12.
[4] Schneider JA, Arvanitakis Z, Leurgans SE, Bennett DA. The neuropathology of probable Alzheimer disease and mild cognitive impairment. Ann Neurol 2009;66:200–8.
[5] Petersen RC, Parisi JE, Dickson DW, Johnson KA, Knopman DS, Boeve BF, et al. Neuropathologic features of amnestic mild cognitive impairment. Arch Neurol 2006;63:665–72.
[6] Auer S, Reisberg B. The GDS/FAST staging system. Int Psychogeriatr 1997;9(Suppl 1):167–71.
[7] Reisberg B, Ferris SH, de Leon M, Crook T. Global Deterioration Scale (GDS). Psychopharmacol Bull 1988;24:661–3.
[8] Reisberg B, Gauthier S. Current evidence for subjective cognitive impairment (SCI) as the pre-mild cognitive impairment (MCI) stage of subsequently manifest Alzheimer's disease. Int Psychogeriatr 2008;20:1–16.
[9] Reisberg B, Shulman MB, Torossian C, Leng L, Zhu W. Outcome over seven years of healthy adults with and without subjective cognitive impairment. Alzheimers Dement 2010;6:11–24.
[10] Arriagada PV, Growdon JH, Hedley-Whyte ET, Hyman BT. Neurofibrillary tangles but not senile plaques parallel duration and severity of Alzheimer's disease. Neurology 1992;42:631–9.
[11] Ohm TG, Müller H, Braak H, Bohl J. Close-meshed prevalence rates of different stages as a tool to uncover the rate of Alzheimer's disease-related neurofibrillary changes. Neuroscience 1995;64:209–17.
[12] Gomez-Isla T, Price JL, McKeel DW Jr, Morris JC, Growdon JH, Hyman BT. Profound loss of layer II entorhinal cortex neurons occurs in very mild Alzheimer's disease. J Neurosci 1996;16:4491–500.

[13] Mosconi L, Brys M, Glodzik-Sobanska L, De Santi S, Rusinek H, de Leon MJ. Early detection of Alzheimer's disease using neuroimaging. Exp Gerontol 2007;42:129–38.
[14] McDonald CR, McEvoy LK, Gharapetian L, Fennema-Notestine C, Hagler DJ Jr, Holland D, et al. Regional rates of neocortical atrophy from normal aging to early Alzheimer disease. Neurology 2009; 73:457–65.
[15] Walhovd KB, Fjell AM, Amlien I, Grambaite R, Stenset V, Bjørnerud A, et al. Multimodal imaging in mild cognitive impairment: metabolism, morphometry and diffusion of the temporal-parietal memory network. Neuroimage 2009;45:215–23.
[16] Fjell AM, Westlye LT, Amlien I, Espeseth T, Reinvang I, Raz N, et al. High consistency of regional cortical thinning in aging across multiple samples. Cereb Cortex 2009;19:2001–12.
[17] Smith SM, Jenkinson M, Johansen-Berg H, Rueckert D, Nichols TE, Mackay CE, et al. Tract-based spatial statistics: voxelwise analysis of multi-subject diffusion data. Neuroimage 2006;31:1487–505.
[18] Song SK, Sun SW, Ramsbottom MJ, Chang C, Russell J, Cross AH. Dysmyelination revealed through MRI as increased radial (but unchanged axial) diffusion of water. Neuroimage 2002;17:1429–36.
[19] Wozniak JR, Lim KO. Advances in white matter imaging: a review of in vivo magnetic resonance methodologies and their applicability to the study of development and aging. Neurosci Biobehav Rev 2006; 30:762–74.
[20] Concha L, Gross DW, Wheatley BM, Beaulieu C. Diffusion tensor imaging of time-dependent axonal and myelin degradation after corpus callosotomy in epilepsy patients. Neuroimage 2006;32:1090–9.
[21] Sjobeck M, Haglund M, Englund E. White matter mapping in Alzheimer's disease: a neuropathological study. Neurobiol Aging 2006; 27:673–80.
[22] Hyman BT, Van Hoesen GW, Kromer LJ, Damasio AR. Perforant pathway changes and the memory impairment of Alzheimer's disease. Ann Neurol 1986;20:472–81.
[23] Chua TC, Wen W, Slavin MJ, Sachdev PS. Diffusion tensor imaging in mild cognitive impairment and Alzheimer's disease: a review. Curr Opin Neurol 2008;21:83–92.
[24] Stebbins GT, Murphy CM. Diffusion tensor imaging in Alzheimer's disease and mild cognitive impairment. Behav Neurol 2009;21:39–49.
[25] Fjell AM, Westlye LT, Greve DN, Fischl B, Benner T, van der Kouwe AJ, et al. The relationship between diffusion tensor imaging and volumetry as measures of white matter properties. Neuroimage 2008;42:1654–68.
[26] Salat DH, Tuch DS, van der Kouwe AJ, Greve DN, Pappu V, Lee SY, et al. White matter pathology isolates the hippocampal formation in Alzheimer's disease. Neurobiol Aging 2010;31:244–56.
[27] Folstein MF, Folstein SE, McHugh PR. "Mini-mental state". A practical method for grading the cognitive state of patients for the clinician. J Psychiatr Res 1975;12:189–98.
[28] Wallin A, Edman A, Blennow K, Gottfries CG, Karlsson I, Regland B, et al. Stepwise comparative status analysis (STEP): a tool for identification of regional brain syndromes in dementia. J Geriatr Psychiatry Neurol 1996;9:185–99.
[29] Royall DR, Mahurin RK, Gray KF. Bedside assessment of executive cognitive impairment: the executive interview. J Am Geriatr Soc 1992;40:1221–6.
[30] Kiernan RJ, Mueller J, Langston JW, van Dyke C. The Neurobehavioral Cognitive Status Examination: a brief but differentiated approach to cognitive assessment. Ann Intern Med 1987;107:481–5.
[31] Morris JC. Clinical dementia rating: a reliable and valid diagnostic and staging measure for dementia of the Alzheimer type. Int Psychogeriatr 1997;9(Suppl 1):173–6. discussion 177–8.
[32] Nordlund A, Rolstad S, Hellstrom P, Sjogren M, Hansen S, Wallin A. The Goteborg MCI study: mild cognitive impairment is a heterogeneous condition. J Neurol Neurosurg Psychiatry 2005;76:1485–90.
[33] Fjell AM, Walhovd KB, Amlien I, Bjornerud A, Reinvang I, Gjerstad L, et al. Morphometric changes in the episodic memory network and tau pathologic features correlate with memory performance in patients with mild cognitive impairment. AJNR Am J Neuroradiol 2008;29:1183–9.
[34] Fischl B, Salat DH, Busa E, Albert M, Dieterich M, Haselgrove C, et al. Whole brain segmentation: automated labeling of neuroanatomical structures in the human brain. Neuron 2002;33:341–55.
[35] Fischl B, van der Kouwe A, Destrieux C, Halgren E, Segonne F, Salat DH, et al. Automatically parcellating the human cerebral cortex. Cereb Cortex 2004;14:11–22.
[36] Desikan RS, Ségonne F, Fischl B, Quinn BT, Dickerson BC, Blacker D, et al. An automated labeling system for subdividing the human cerebral cortex on MRI scans into gyral based regions of interest. Neuroimage 2006;31:968–80.
[37] Smith SM, Jenkinson M, Woolrich MW, Beckmann CF, Behrens TE, Johansen-Berg H, et al. Advances in functional and structural MR image analysis and implementation as FSL. Neuroimage 2004;23(Suppl 1):S208–19.
[38] Woolrich MW, Jbabdi S, Patenaude B, Chappell M, Makni S, Behrens T, et al. Bayesian analysis of neuroimaging data in FSL. Neuroimage 2009;45:S173–86.
[39] Jenkinson M, Smith S. A global optimisation method for robust affine registration of brain images. Med Image Anal 2001;5:143–56.
[40] Rueckert D, Sonoda LI, Hayes C, Hill DL, Leach MO, Hawkes DJ. Nonrigid registration using free-form deformations: application to breast MR images. IEEE Trans Med Imaging 1999;18:712–21.
[41] Smith SM, Nichols TE. Threshold-free cluster enhancement: addressing problems of smoothing, threshold dependence and localisation in cluster inference. Neuroimage 2009;44:83–98.
[42] Stenset V, Bjornerud A, Fjell AM, Walhovd KB, Hofoss D, Due-Tonnessen P, et al. Cingulum fiber diffusivity and CSF T-tau in patients with subjective and mild cognitive impairment. Neurobiol Aging 2011;32:581–9.
[43] de la Torre JC. Cerebrovascular and cardiovascular pathology in Alzheimer's disease. Int Rev Neurobiol 2009;84:35–48.
[44] Selkoe DJ. Cell biology of protein misfolding: the examples of Alzheimer's and Parkinson's diseases. Nat Cell Biol 2004;6:1054–61.
[45] Yukie M, Shibata H. Temporocingulate interactions in the monkey. In: Vogt B, ed. Cingulate Neurobiology and Disease. Oxford, UK: Oxford University Press; 2009. p. 145–62.
[46] Fennema-Notestine C, Hagler DJ Jr, McEvoy LK, Fleisher AS, Wu EH, Karow DS, et al. Structural MRI biomarkers for preclinical and mild Alzheimer's disease. Hum Brain Mapp 2009;30: 3238–53.
[47] Vickers JC, King AE, Woodhouse A, Kirkcaldie MT, Staal JA, McCormack GH, et al. Axonopathy and cytoskeletal disruption in degenerative diseases of the central nervous system. Brain Res Bull 2009;80:217–23.
[48] Acosta-Cabronero J, Williams GB, Pengas G, Nestor PJ. Absolute diffusivities define the landscape of white matter degeneration in Alzheimer's disease. Brain 2010;133:529–39.